OBSERVATIONS WITH THE UNIVERSITY OF WISCONSIN ARCTIC HIGH SPECTRAL RESOLUTION LIDAR

Edwin W. Eloranta, Igor A. Razenkov, Joesph P. Garcia, and James Hedrick

University of Wisconsin, 1225 W. Dayton St., Madison, WI, USA, E-mail:eloranta@lidar.ssec.wisc.edu

ABSTRACT

The University of Wisconsin Arctic High Spectral Resolution Lidar has acquired over 6000 hours of data during shakedown testing. Examples of this data are presented to illustrate HSRL measurement capabilities.

1. INTRODUCTION

Climate models suggest that the Arctic climate is particularly sensitive to perturbation by increasing levels of greenhouse gases. This sensitivity seems to be verified by measurements which show that the Arctic is warming faster than any other part of the globe. However, comparison of many climate models show wide variations in predictions for future warming. Studies of these differences show that the greatest source of uncertainty relates to the modeling of clouds. The models use different parameterizations to describe clouds resulting in very different cloud predictions. Unfortunately, very little observational data is available for verification. Arctic cloud observations have been limited by several factors including: 1) the lack of observers, 2) the difficulty of seeing clouds during the long Arctic night, 3) a lack of visual and temperature contrast between clouds and the snow surface, which impedes satellite cloud retrievals, and 4) the inconsistent reporting of diamond dust precipitation.

Modelers require information on cloud optical depth, cloud altitudes and cloud phase. Operation of the NOAA DABUL lidar on an ice breaker frozen into the Arctic ice pack during the SHEBA experiment illustrated the utility of lidar data in Arctic cloud studies[1]. DABUL observed incredibly complex mixed-phase cloud structures with intermixed pockets of pure water and ice. While DABUL provided much useful information data analysis was hampered by limitations common to all conventional backscatter lidars. The inability to correct signals for attenuation without a priori assumptions makes it impossible to derive reliable optical depth, or backscatter cross section profiles. This ambiguity also forces laborious hand analysis of the data.

The University of Wisconsin has constructed a High Spectral Resolution Lidar (HSRL) for long-term Arctic cloud studies. This system, which is designed to operate as a minimally-tended Internet appliance, provides abso-

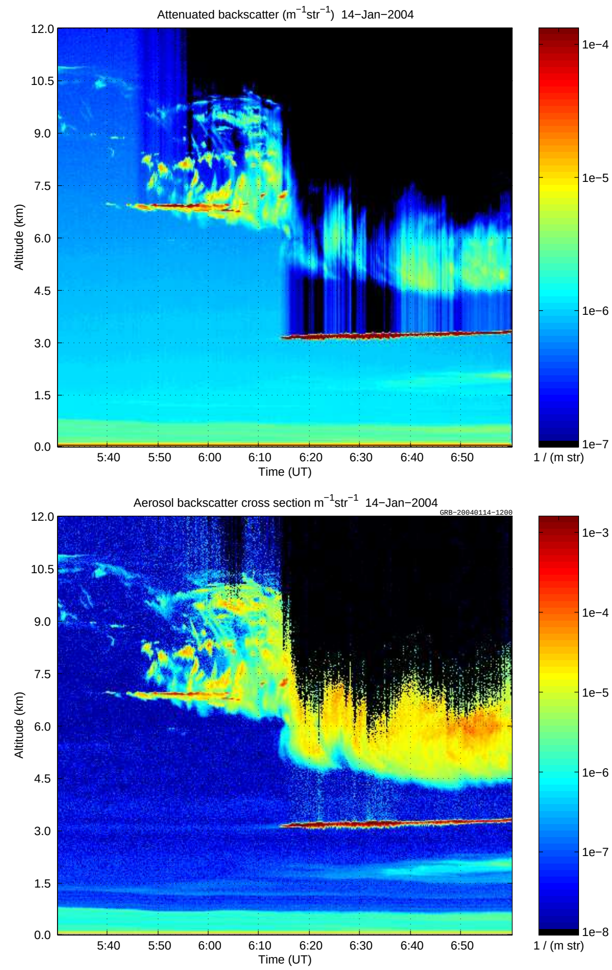

Figure 1. The r-squared, energy, and overlap corrected lidar signal measured in the combined channel(upper panel) and the HSRL derived backscatter cross section (lower panel). Data was acquired between 6:30 and 7:00 UTC on 14 January 2004. This upper panel image is identical to that obtained from a well calibrated conventional backscatter lidar. In the conventional image the lower cloud shadows the cirrus above, while the HSRL measurements are unaffected until the signals are total extinguished.

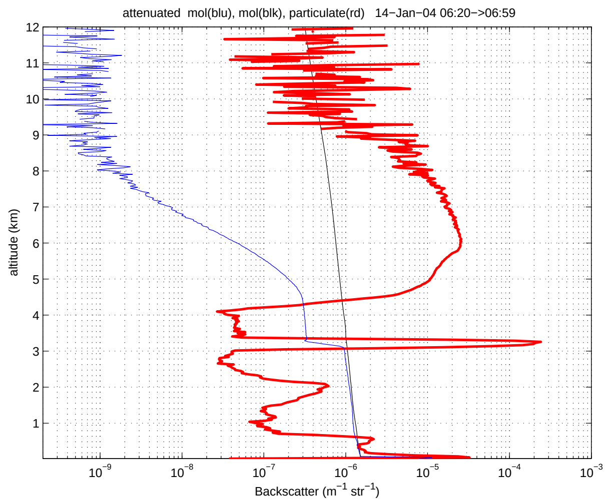

Figure 2. The aerosol backscatter cross section (right curve with peak at 3 km), the attenuated molecular cross section (left) and the Rayleigh backscatter cross section computed from a Radiosonde temperature profile (slowly decreasing center curve). Profiles are an average of data measured between 6:20 and 7:00 UTC on 14 January 2004.

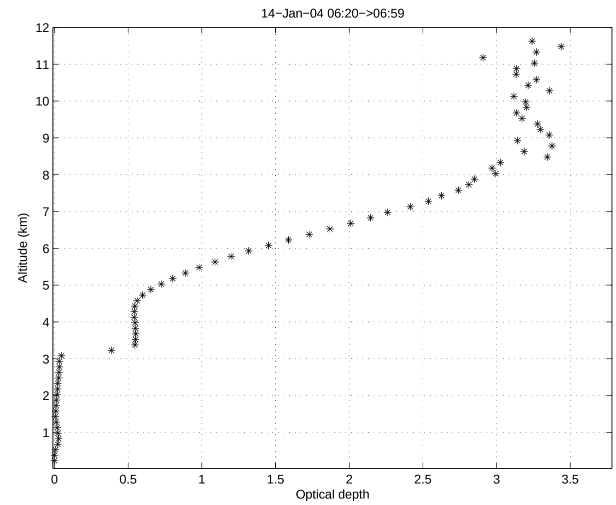

Figure 3. Optical depth profile computed from data acquired between 6:20 and 7:00 UTC on 14 January 2004.

lutely calibrated profiles of backscatter cross section, optical depth and depolarization[2][3] [4]. It requires only electrical power, an Internet connection, and a zenith facing window for operation. All control and data transfer is accomplished via the Internet. No routine on site attention is required other than cleaning of the window. Use of a 4 kHz repetition rate laser and expansion of the transmitted beam through a 40 cm telescope reduces the transmitted energy density to eye-safe levels, making it possible to look directly into the output beam without hazard. A 45μrad. angular field-of-view coupled with a 8 GHz bandwidth etalon filter reduces background noise to very low levels. A high-dynamic range photon counting data system provides profiles with 7.5 m range resolution up to a maximum altitude of 30 km. Detector gain changes are not required in response to changing weather; conditions ranging from the clear atmosphere to dense low-altitude water clouds can be accommodated. This paper describes measurements derived with the new HSRL during shakedown testing in our Madison, WI laboratory.

2. HSRL DATA

The new HSRL is currently installed under a zenith-facing window on the top of our laboratory. The system operates 24-hours/day and more than 6000 hours has been acquired during testing. Data is automatically transfered in real time from the lidar to our archive computer via a fault-tolerant client-server application where it is stored as netcdf files on a 1-terabyte raid disk system. All data can be accessed through a publicly accessible web site: 'lidar.ssec.wisc.edu'. Real time access is provided by a web tool which computes images and profiles on demand using: 1) the raw data, 2) weather service Radiosonde temperature profiles, and 3) system calibration data. The time and altitude interval for the data can be specified. Data may also be searched via web pages which provide a complete month of 12-hour thumbnail images of the backscatter cross section between the surface and 15 km. Clicking on an image provides a full screen version of the backscatter cross section and the depolarization image. An online system log book provides information about system maintenance and software modifications. A web tool is provided to display system housekeeping data as well. We are also preparing web routines to process data on demand and deliver the output to users in netcdf format.

Figure 1 shows images acquired on 14-January 2004 between 5:30 and 7:00 UTC. These images compare a standard lidar image of the attenuated backscatter cross section with a backscatter cross section image derived for the same period. In the conventional image (upper panel), cirrus cloud measurements are corrupted by attenuation. Distinct shadows appear in the image and the attenuated backscatter cross section values depend on the presence or absence of underlying water clouds. The HSRL measured backscatter cross section (lower panel) eliminates this dependence. Although attenuation in the lower cloud reduces the maximum altitude which can be observed, the attenuation does not affect the backscatter values where signal is present. Because the HSRL scattering cross section measurements are computed from the relative intensity of the molecular backscatter and particulate backscatter at each altitude, the values are independent of attenuation at lower levels. This provides another advantage; calibration is insensitive to dirt, water or snow on the output window.

Figure 2 shows backscatter cross section profiles representing an average over the period between 6:20 and 7:00

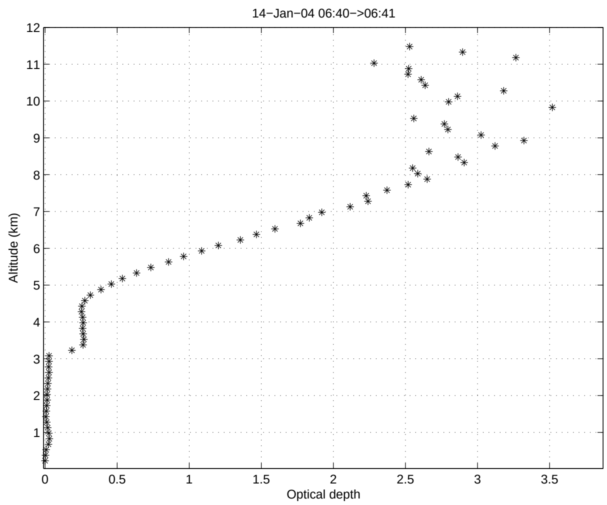

Figure 4. Optical depth profile computed from a one-minute average observed between 6:40 and 6:41 UT on 14 January 2004.

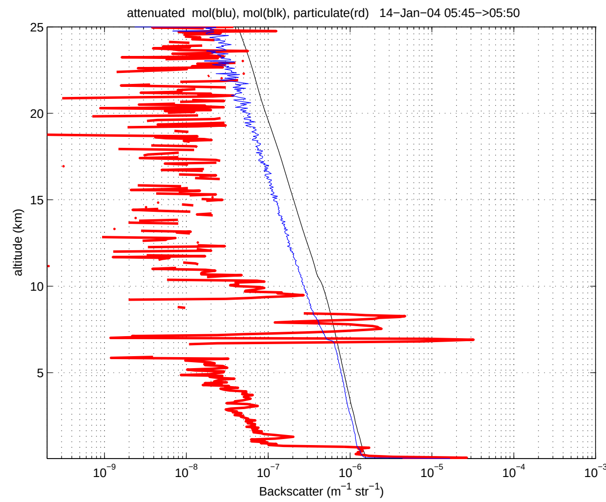

Figure 5. The aerosol backscatter cross section (noisy curve), the attenuated molecular cross section (center curve) and the Rayleigh backscatter cross section computed from a Radiosonde temperature profile(smooth on right). Profiles are an average of data measured between 5:45 and 5:50 UTC on 14 January 2004.

UTC. The Rayleigh backscatter cross section computed from a Radiosonde temperature profile is shown along with the derived particulate scattering cross section and the measured attenuated-molecular scattering cross section. Whereas, during this period, the 12.5-second averaging used to prepare figure 1 does not show clouds above 7.5 km, the 40-minute average profile extends to the top of the cirrus cloud.

Useful profiles begin exceptionally close to the lidar; detectors quickly recover from an initial transient and data is valid above 75 m. This illustrates effective isolation of the detectors from scattered laser light. Detector overload is often a problem in lidars which use the same telescope to receive and transmit. The molecular channel detector is exposed to approximately 10 photons, which have been scattered from optics as the laser pulse exits the system. The combined-channel photomultiplier, which is not protected by the iodine absorption filter, is exposed to approximately 200,000 photons, which, after taking into account the 5% quantum efficiency of the photomultiplier, produce approximately 10,000 photoelectons.

Low-attitude observations are particularly important in the Arctic where persistent stratus layers with cloud bases below 1 km are frequently observed. The backscatter cross section measurement is computed from the ratio of the molecular and combined channel signals so that it is independent of any range-dependent geometric corrections. However, this is not true for the attenuated-molecular cross section profile. The angular field-of-view of the lidar is only 45μrad and the raw HSRL signals depart strongly from the standard r^{-2} dependence at altitudes below 5 km. This effect is measured as part of the system calibration and removed during data processing. These geometric corrections have proven to be very stable, reflecting the advantage of using a common telescope to transmit and receive. We had planned to measure the geometric correction by scanning the telescope focus while recording data. The lidar includes a computer-actuated focus control which can provide micron-level adjustments in the position of the telescope secondary mirror. A comparison of the molecular-channel, near-range, signal with the system focused at near-range to the same signal with the lidar at its operating focus was going to be used to provide the geometric correction. However, it has proven adequate to compute the geometric correction factor from a comparison of the molecular signal measured during very clear weather with the molecular lidar return predicted from a measured temperature profile.

Figure 3 shows the optical depth measured as a function of altitude above a reference point at 75 meters. This is computed from the ratio of the computed molecular cross section and the observed attenuated molecular cross section shown in figure 2. Notice the correspondence between attenuation of the molecular return shown in figure 2 and the optical depth curve. The attenuation caused by the 3-km water cloud and the 5 to 9 km cirrus clouds are directly reflected in the optical depth curve. In this case the total optical depth of the atmosphere is approximately 3.2. For short averaging times, the maximum optical depth which can be measured with the lidar is determined by photon statistics; the penetration depth increases with averaging time. For long averaging times, the maximum optical depth is currently limited to values less than 4 by detector after-pulse contributions to the molecular signal. Figure 4 shows an optical depth measurement derived from a one-minute average. In this case, the curve becomes noisy for optical depths greater than 2.5.

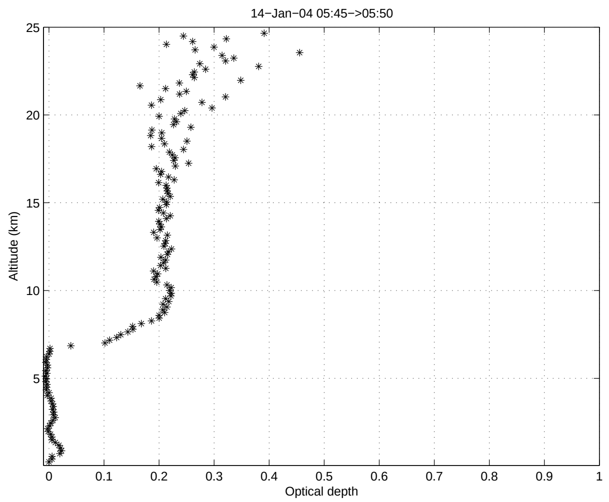

Figure 6. Optical depth profile observed between 5:45 and 5:50 on 14 January 2004.

Figure 5 provides an example of backscatter cross section profiles from a much cleaner atmosphere. This five-minute average has been computed using data from figure 1 between 5:45 and 5:50 UTC. It extends to an altitude of 25 km. Sufficient signal is observed to provide good signal-to-noise ratios in the attenuated molecular profile up to approximately 20 km. This is verified in the optical depth profile, which is presented in figure 6. An optical depth of 0.2 is measured in the thin cirrus cloud between 7 and 10 km. Fluctuations in the optical depth profile below the cloud reflect errors in the geometric correction and the temperature profile used to compute the molecular backscatter cross section. The temperature profile was obtained from a Radiosonde launched approximately 150 km from our laboratory.

ACKNOWLEDGMENTS

This research was supported by National Science Foundation Grant OPP-9910304,

REFERENCES

[1] Intrieri, J. M.,M. D. Shupe, T. Uttal, B. J. McCarty An annual cycle of Arctic cloud characteristics observed by radar and lidar at SHEBA. *J. Geophys. Res. (C Oceans)*, 107: 2002.

[2] Razenkov, I. A., E. W. Eloranta, J. P. Hedrick, R. E. Holz, R. E. Kuehn, and J. P. Garcia. A High Spectral Resolution Lidar Designed for Unattended Operation in the Arctic. *Proc. ILRC21, 57-60, 2002*

[3] Pirronen, P. A high spectral resolution lidar based on an iodine absorption filter Ph.D. thesis, Univ. of Joensuu, Joensuu, Finland, pp 113, 1994.

[4] Grund, C. J. and E. W. Eloranta The University of Wisconsin High Spectral Resolution Lidar *Optical Engineering*, 30: 6-12, 1991.